Nanomed Res J 2(3):171-178, Summer 2017

RESEARCH ARTICLE

# Biofabrication of manganese nanoparticle using *Aegle marmelos* fruit extract and assessment of its biological activities

***Keerthana Sivanesan, Priyanga Jayakrishnan, Sirajunnisa Abdul Razack, Pavitra Sellaperumal, Geethalakshmi Ramakrishnan and Renganathan Sahadevan****

*Centre for Biotechnology, Anna University, Chennai-600025, Tamilnadu, India*

**ARTICLE INFO**

***Article History:***
*Received 09 July 2017*
*Accepted 18 September 2017*
*Published 29 September 2017*

***Keywords:***
*Aegle marmelos*
*Manganese nanoparticle*
*Characterization studies*
*Anti-biofilm*
*Antioxidant*

**ABSTRACT**

**Objective(s):** The present investigation dealt with the biological production of manganese nanoparticles using ***Aegle marmelos*** fruit and assessing the antioxidant and antibiofilm activities.

**Methods:** The nanoparticles were produced using the fruit extract of ***Aegle marmelos*** as the reducing agent with potassium permanganate as the substrate. Manganese nanoparticles synthesized were characterized by UV-Vis spectroscopy, Scanning Electron Microscopy, FT-IR spectroscopy and X Ray Diffractometry. Antibiofilm and antioxidant activities of the nanoparticles were assessed by DPPH and crystal violet staining methods respectively and were statistically analysed using SPSS software.

**Results:** The characterisation study reported that the average crystallite size of the formed nanoparticle was 23.7nm. The results indicated that biofilms of gram positive and gram negative bacteria were inhibited at 80 and 100 µg of nanoparticles/ml respectively showing more activity against gram positive bacterial biofilms. The highest activity was observed against ***E.coli*** as 1.217±0.43 at 80 µg/ml and ***B.subtilis*** as 1.705±0.37 at 100 µg/ml. Maximum activity of nanoparticle against reactive oxygen species was found to be at a concentration of 5mg/ml as 27.31±0.03%.

**Conclusions:** This study demonstrated that the biologically synthesized manganese nanoparticles are environment-friendly with its potential applications against pathogens and could be implied for various other biological purposes.

**How to cite this article:**
*Sivanesan K, Jeyakrishnan P, Abdul Razack S, Sellaperumal P, Ramakrishnan G and Sahadevan R. Biofabrication of manganese nanoparticle using aegle marmelos fruit extract and assessment of its biological activities. Nanomed Res J, 2017; 2(3):171-178. DOI: 10.22034/nmrj.2017.03.005*

## INTRODUCTION

Synthesis of nanoparticle gained importance due to their unique optical, electronic, mechanical, magnetic and chemical properties compared to the bulk materials. These special and unique properties could be attributed to their small size and large surface area [1]. In particular, nanocrystals of metal oxide are considered valuable due to their application in medicine, healthcare, catalysis, energy storage, magnetic data storage, sensors, ferrofluids and various other fields. Metal oxide nanoparticles have wide applications as drug delivery systems for treatment and diagnosis, semiconductor, thermoelectric material and in environmental decontamination process [2]. The metal oxide nanoparticles such as manganese oxide, zinc oxide, and titanium dioxide are not only stable but also safe to humans [3]. Manganese dioxide ($MnO_2$) is one of the most attractive inorganic materials [4]. The manganese oxide nanoparticles have the larger surface area, and these positively charged particles have a strong interaction with negatively charged particles. Compared to other metal oxide nanoparticles, $MnO_2$ has the advantage of easily prepared from readily available

* Corresponding Author Email: *rengsah@rediffmail.com*

solvents [3]. Several physiochemical techniques are commonly followed to synthesise nanoparticles which include physical vapor deposition, chemical vapor deposition, aerosol processing, Sol-Gel method, reverse micelle method and mechanical alloying or milling [5]. Apart from being non-toxic and environmentally friendly when compared to the physiochemical methods, biogenic synthesis produce large quantities of nanoparticles that are free of contamination and exhibit better defined size and morphology than few other physiochemical methods [6]. Conventional physical and chemical methods have several disadvantages including usage of hazardous and expensive chemicals and negative impact on the environment. Hence biogenic synthesis of nanoparticles from living sources are of recent interest which offers flexible, biocompatible, low cost, non-toxic and environmentally benign procedure [2, 7]. Plants are considered to be a major source for the development of new drugs because of its non-toxicity, affordability and fewer side effects. *Aegle marmelos*, the golden apple, belongs to the family Rutaceae and it is the only member of the monotypic genus *Aegle* [8]. Almost all parts have medicinal value hence it is more commonly used in Indian medicine for relieving constipation, dysentry, diarrhoea, peptic ulcer and respiratory functions [9]. More than 100 compounds have been isolated from various parts of the tree including phenols, flavanoids, alkaloids, terpenoids, and steroids. These compounds possess great pharmacological activity against various chronic diseases such as cancer, cardiovascular diseases and gastrointestinal disorders [10].

Synthesis of various kinds of nanoparticles are carried out using different biomass such as bacteria, actinomycetes, yeasts, filamentous fungi, lichen, algae and plants [7]. Plant extract mediated synthesis is readily scalable and less expensive than microbial mediated synthesis which is quite expensive which involves the production of microorganisms. The plant extract is simply mixed with a solution of metal salt at room temperature, and the synthesis occurs within few minutes [6]. Using plant extract for synthesis is considered more efficient than microbial production as the extracts have various biologically active chemicals that can serve as reducing and capping agents and can occur at the lesser time under normal conditions like relatively low temperature, optimum pressure [11]. Nano- $MnO_2$ has been widely used in various areas and recently reported to have a good bactericidal effect [3]. New reports are put forward on utilizing plant sources against various pathogens especially those that are multidrug resistant and biofilm forming [12]. $MnO_2$ nanoparticles prepared from plant extracts as reducing agents show significant biological activities. The present research was attempted to synthesise manganese oxide nanoparticles using fruit extract of *Aegle marmelos*, characterize them and assess the anti-biofilm forming ability and antioxidant activities of the nanoparticles. From an extensive literature survey, it is noted that this is the first report on synthesizing $MnO_2$ nanoparticles from *Aegle marmelos*.

## MATERIALS AND METHODS

*Sample collection*

The ripened fruits of A. marmelos were taken for the study. The samples were collected from the local areas of Chennai, Tamilnadu, India in sterile air tight containers, transferred to the laboratory and stored at 4˚C until use. The fruits with hard outer shells are washed with sterile distilled water and later with a surfactant, 10% Tween20. Outer shells were broken, and the pulp was collected in sterile screw capped bottles under aseptic conditions and stored at 4˚C until for further experimentation.

*Preparation of fruit extract*

A quantity of 2g of the fruit sample was taken and added to 10ml of different solvents namely isopropanol, acetone and water. The mixture was stored for 10 days under non aerated and non-agitated conditions and in the dark. After incubations, the mixtures were centrifuged at 10,000rpm for 10min at 4˚C. The supernatant was collected and stored for further studies.

*Phytochemical analyses*

Phytochemical analyses were performed to identify the best solvent which could extract the maximum of the phytochemicals that act as reducing and capping agents.

*Test for alkaloids*

Meyer's test: A volume of 0.5ml of the extract was mixed with few drops of Meyer's reagent (mercuric chloride and potassium iodide in water) and checked for cream color precipitation. Wagner's

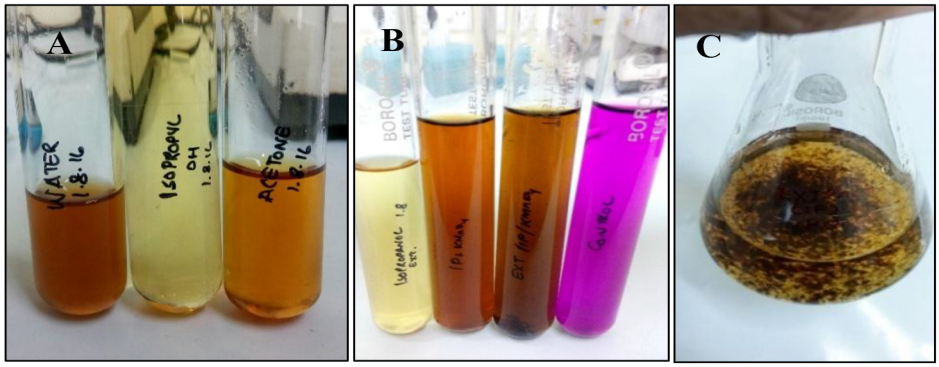


**Fig. 1.** (A) Solvent extraction, (B) synthesis of nanoparticle, (C) brown precipitation confirming synthesis of MnO2 nanoparticle

test: A volume of 0.5 ml of extract was taken and Wagner's reagent (Iodine and potassium iodide in water) was added in drops and checked for reddish brown coloration/precipitation.

*Test for proteins*

Bradford's test: A volume of 0.5ml extract was added with few drops of Bradford's reagent and checked for blue coloration

*Test for carbohydrates*

To a volume of 0.5ml of the extract, few drops of Fehling's reagent was added and checked for its red color precipitate.

*Test for saponins*

Froth test: A volume of 0.5 ml of extract was diluted with twice the volume of distilled water and checked for froth formation upon mixing. Saponin is tested positive if the froth persists for a longer duration and is negative when it disappears immediately after shaking.

*Test for phenols*

Ferric chloride test: 3-5 drops of 5% ferric chloride solution was added to 0.5 ml of extract and checked for red, blue, green or purple coloration

*Test for cholesterol*

To a volume of 1 ml of extract, 2 ml of acetic acid was added followed by few drops of concentration. $H_2SO_4$ and checked for bluish green coloration

*Synthesis of $MnO_2$ nanoparticles*

A volume of 1 ml of the fruit extract was added to 9 ml of 1M potassium permanganate ($KMnO_4$) and left overnight. Color change from magenta pink to dark brown indicates the formation of manganese oxide nanoparticles. The nanoparticles were then centrifuged at 10000 rpm for 10min. The pellet was collected and dried in hot air oven at 60˚C overnight. The dried pellet was heated in muffle furnace at 700˚C for 7h. The powdered nanoparticles were stored in capped vials for further analyses.

*Characterization of nanoparticles*

The $MnO_2$ nanoparticles were characterized to confirm the formation and analyse its shape and size. Preliminary confirmation was carried out using UV-Visible spectrophotometer (Model: G10S, Thermo Fisher Scientific Ltd., USA). A quantity of 0.01g of nanoparticle powder sample was dispensed in 3ml distilled water and was scanned at a range of wavelengths between 200 and 700nm for checking the maximum absorbance with distilled water as the blank.

The crystallite size was determined by X Ray Diffraction studies using an X-Ray diffractometer (XPert Pro) running at 30mA and 40kV. A quantity of 1mg sample was taken, spread on a glass slide and heated at 4000C to obtain a thin film and diffraction intensitites were obtained by scanning from 10 to 80 degrees 2θ angle. The size was calculated from the spectrum using the Debye-Schrerr's equation

$$D = (k\lambda)/(\beta\cos\theta)$$

where D is the crystallite size of the nanoparticle, k is the shape factor, λ is the wavelength, θ is the Bragg's angle and β is the line width (FWHM) in radians. The shape of the nanoparticles was determined by scanning electron microscopy (Model: Carl Zeiss, Germany).

The functional groups present in $MnO_2$ nanoparticles were identified using an FT-IR spectroscope (Model: Spectrum RX 1, Perkin Elmer). A quantity of 150mg KBr was mixed with 50mg of the analyte, pressed to a fine thin disc using a hydraulic press which was then used as the sample to analyse in spectroscope between wavenumbers ranging from 4000-400/cm.

*Antioxidant activity of $MnO_2$ nanoparticles*

The antioxidant activity of $MnO_2$ nanoparticles was evaluated on the basis of the free radical scavenging effect of 1, 1- diphenyl 2- picrylhydrazyl (DPPH) [13]. In brief, sample solutions at various concentrations of mg/ml were made upto to 1 ml with distilled water. 1 ml of DPPH solution (0.004% in methanol) was added to 1 ml of sample and standard solutions in the ratio 1:1. After incubating the solutions for 30 min at dark, the absorbance was read at 517nm. Vitamin C and distilled water with DPPH were used as the reference and blank respectively. Percent scavenging ability was calculated using the formula:

Percent (%) scavenging activity = 1 – (A/B) x 100

where, A=(Control OD–Test OD) and B= Control OD.

*Antibiofilm activity of $MnO_2$ nanoparticles*

A standard crystal violet staining procedure was used for the evaluation. 1% crystal violet solution was used for the study. Gram negative microorganisms namely Escherichia coli, Pseudomonas aeruginosa, Enterobacter aerogenes, Klebsiella pneumoniae and Gram positive bacterium Bacillus subtilis and yeast Candida albicans were selected for the study at a concentration of 107 CFU/ml. Biofilm inhibition efficacy of $MnO_2$ NP was tested at concentrations ranging between 0.5 and 2.5mg/ml. Equivolume of culture and nanoparticle solution (50µl each) was added into wells of a 96-well microtitre plate and incubated for three days with the stain (50µl). After incubation, the mixture was discarded and washed thrice with 1X PBS to remove unbound biofilm and debris. Then the wells were decolorized using 100% ethanol and read using a microplate reader (Model: Synergy H1 BIOTEK Microplate Reader, USA) at 625 nm [14].

*Statistical analysis*

All the data for antioxidant and antibiofilm activity carried out in triplicates are expressed as mean±SD. Statistical analysis was done, using SPSS software v.21.0 for Windows, based upon the ANOVA at confidence level 95%.

## RESULTS AND DISCUSSION

*$MnO_2$ nanoparticle synthesis*

The present study is on the synthesis of $MnO_2$ nanoparticles using the fruit extract of *Aegle marmelos*. The phytochemical compounds were found to be extracting at its maximum when isopropanol was used as the organic solvent, as compared to water and acetone (Figure 1A). Using this extract, $MnO_2$ nanoparticle synthesis was carried out (Figure 1B,1C). Compared to the use of whole plant and plant extract, plant extract mediated synthesis is simpler and is an interesting area of focus. Plant extract may act both as reducing and capping agents. The biogenic synthesis leads to the formation of capped nanoparticles due to the presence of phytochemicals. Capping reduces aggregation and provides stability to the

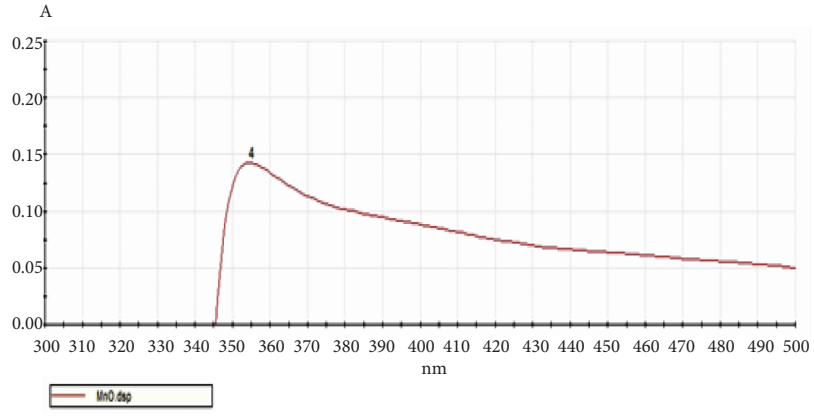


**Fig. 2.** Represents the UV-Visible spectrogram

nanosystems. This increases the biocompatibility [2, 7]. The efficiency of capping and reducing capacities depend on the source of the plant being used. This is because of the presence of different concentrations of organic reducing agents in plants [6].

*Characterisation studies*

The preliminary characterization of MnO nanoparticle was carried out using UV-Visible spectrophotometer. The spectrum showed an intense peak at 355nm which confirmed the presence of MnO nanoparticles (Figure 2). The range was in complete agreement with several reports that characterized the nanoparticles [4, 15]. The peak observed due to the phenomenon referred to as Surface Plasmon Resonance (SPR) where the oscillation of free electrons resonate with the light passing through the sample which leads to high plasmon frequency [16, 17].

The crystallite size of the $MnO_2$ nanoparticle was determined through XRay Diffraction studies. Figure 3 represents the graph showing peaks at obtained for the synthesized nanoparticle. From the illustration, the average diameter of the nanoparticle was 23.7 nm, calculated using Debye-Schrerr's equation and confirmed that the particle was nanocrystalline. The nanoparticles upon calcination at higher temperatures at 400˚C might have attributed to changes in structure bringing out higher symmetry [18]. Calcination is done for thermal decomposition of solid substances at higher temperatures and aids in increasing the adsorbing sites, i.e., porosity, on the material.

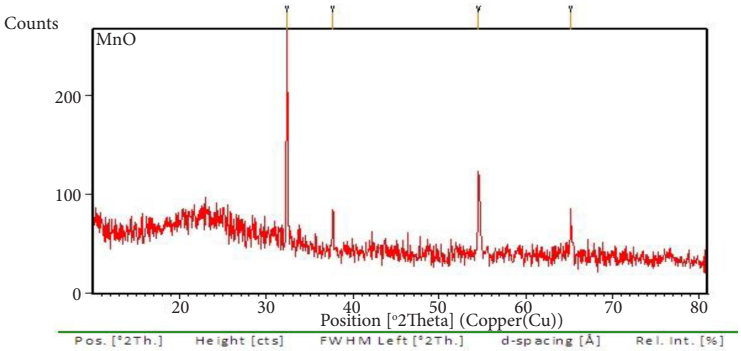


| Pos. [°2Th.] | Height [cts] | FWHM Left [°2Th.] | d-spacing [Å] | Rel. Int. [%] |
|---|---|---|---|---|
| 32.3974 | 214.18 | 0.1476 | 2.76352 | 100.00 |
| 37.6919 | 39.78 | 0.1476 | 2.38662 | 18.58 |
| 54.5918 | 88.62 | 0.2460 | 1.68112 | 41.37 |
| 65.1842 | 50.03 | 0.1476 | 1.43123 | 23.36 |

**Fig. 3.** Illustrates the XRD graph of the MnO2 nanoparticle

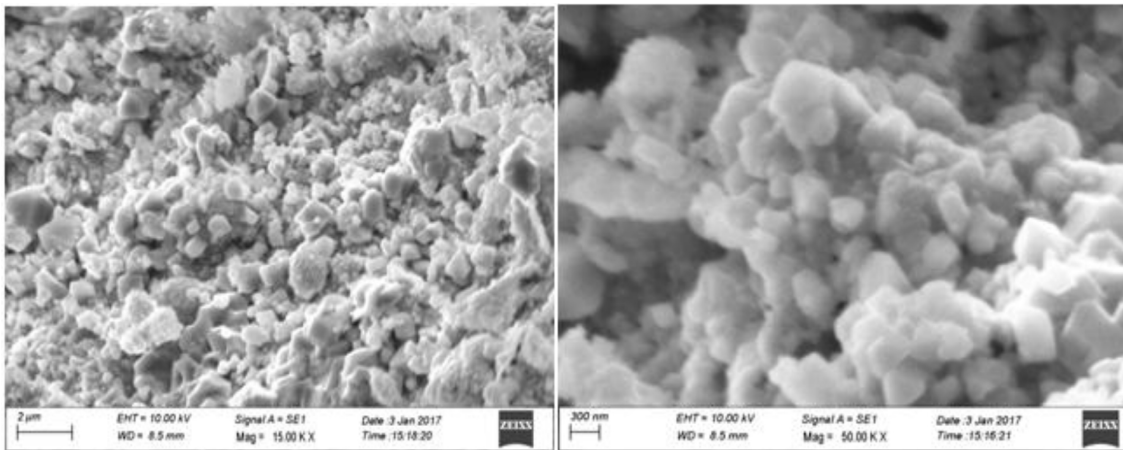


**Fig. 4.** Illustrates the SEM images of $MnO_2$ nanoparticle

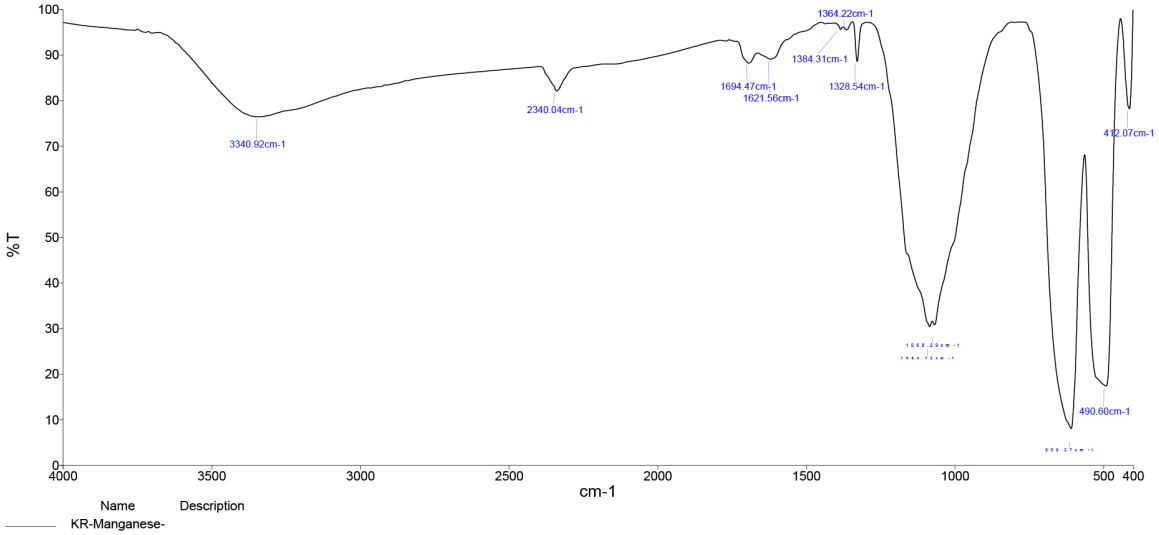


**Fig. 5**. represents the FTIR spectrogram of the MnO nanoparticle

The structural morphology of the nanoparticle was determined using scanning electron microscopy (Figure 4). The biofabricated nanoparticles were mostly smooth edged and tetragonal in shape with smaller particles overlapping each other to form agglomerates exhibiting irregular shapes.

FTIR spectroscopy is performed to determine the organic and inorganic components in the sample. The spectrum showed peaks ranging between 4000–400 $cm^{-1}$. The observed peaks for the $MnO_2$ nanoparticle were 3340.92, 2340.04, 1694.47, 1621.56, 1364.22, 1384.31, 1328.54, 1068.29, 1084.72, 608.27, 490.60 and 412.72 (Figure 5). The absorption peak at 3340.92 denoted the stretching collision of –OH group. The peak at 2340.04 represented –C–H stretching and 1694.47 depicted strong –C=O stretching bond in the nanopowder. The absorption peak at 1621.56 showed O–H stretching of Mn atom. An absorption peak at 1384.31 represented surface OH groups of Mn–OH. An absorption peak at 1068.29 denoted –C–O stretching and 1084.72 represented the presence of amine group which illustrated the involvement of protein molecules in the synthesis of nanoparticles [4, 19]. Oxides and hydroxides of metal nanoparticles generally show absorption peak below 1000 nm due to inter-atomic vibrations [5]. $MnO_2$ possess stronger bonds and weaker vibrations which in turn lower the intensity of absorption peaks. The lower absorption peaks at 608.27, 490.60 represented the stretching collision of O–Mn–O which generally lies in the absorption band 600-475 $cm^{-1}$. FTIR spectrum confirmed the formation of $MnO_2$ nanoparticles [4, 19, 20]

**Table 1**. Free radical scavenging activity of $MnO_2$ nanoparticle

| Concentration (mg/ml) | % scavenging activity | |
|---|---|---|
| | Vitamin C | $MnO_2$ nanoparticle |
| 1 | 3.13±0.09 | 7.94±0.03 |
| 2 | 5.49±0.07 | 13.43±0.18 |
| 3 | 25.43±0.08 | 19.03±0.08 |
| 4 | 37.20±0.30 | 22.5±0.16 |
| 5 | 41.6±0.05 | 27.31±0.03 |

*Antioxidant activity of $MnO_2$ nanoparticle*

DPPH assay was carried out to perform free radical scavenging activity of the synthesized nanoparticles (Figure 5). Antioxidants are those macromolecules that could scavenge the free radicals of reactive oxygen species, ie., superoxide anions like hydrogen peroxide, singlet oxygen, and free hydroxyl ions, which are generated by the transfer of one electron [21]. DPPH could be scavenged on accepting one hydrogen or an electron [22]. Thus this activity results in the reduction of stable DPPH radical (purple) to nonradical (yellow) form. This occurs in the dose dependent manner [21].

The study showed that at lower concentrations the activity was higher than the standard, Vitamin C

**Table 2.** Anti biofilm capacity of the biologically synthesized $MnO_2$ nanoparticle

| Organism | Concentration (µg/ml) | | | | | | |
|---|---|---|---|---|---|---|---|
| | control | 20 | 40 | 60 | 80 | 100 | 120 |
| *E.coli* | 1.871±0.31 | 1.653±0.49 | 1.511±0.31 | 1.279±0.33 | 1.217±0.43 | 0.664±0.22 | 0.664±0.26 |
| *B.subtilis* | 0.848±0.21 | 1.438±0.43 | 1.163±0.32 | 1.186±0.54 | 0.77±0.32 | 1.705±0.37 | 1.718±0.39 |
| *Ent.aerogenes* | 1.168±0.24 | 1.153±0.45 | 0.813±0.33 | 0.542±0.55 | 0.487±0.21 | 0.430±0.42 | 0.434±0.44 |
| *P.aeruginosa* | 1.034±0.44 | 1.347±0.66 | 1.266±0.45 | 0.962±0.41 | 0.928±0.31 | 0.849±0.31 | 0.849±0.30 |
| *K.pneumoniae* | 0.436±0.67 | 1.932±0.54 | 1.603±0.80 | 1.217±0.62 | 1.004±0.44 | 0.378±0.58 | 0.378±0.54 |
| Candida sp. | 1.328±0.71 | 0.995±0.76 | 0.757±0.72 | 0.514±0.74 | 1.192±0.34 | 1.191±0.33 | 1.191±0.32 |

but as the concentrations increased the activity gradually increased but not as effective as the standard. Statistical analysis using ANOVA suggested that the model was significant with no differences at 95% confidence level ($p<0.05$). The maximum potential of the nanoparticle to eradicate ROS was found to be at 5mg/ml concentration as 27.31±0.03%. The redox potential of phytochemicals presents in the plant extract play a major role in neutralizing free radicals, quenching singlet and triplet oxygen and decomposing the free radicals. The adsorption of antioxidant material from the extract onto the surface of nanoparticles is believed to be responsible for the antioxidant activity of the nanoparticles.

*Anti-biofilm activity of $MnO_2$ nanoparticle*

Antibiofilm assay was performed to check the efficiency of manganese nanoparticles in preventing the formation of biofilm by selected bacterial genera and Candida sp. Biofilm inhibition efficacy of $MnO_2$ NP was tested at concentrations ranging between 20 and 120µg/ml. The results indicated that 100µg/ml showed the maximum inhibition of the biofilms formed by Gram negative bacteria and 80µg/ml was found to be inhibiting Gram positive biofilms at its best (Table 2). The statistical analysis revealed that there was no much deviations seen at the concentrations of 100 and 120 µg/ml ($p<0.05$) in each case of the organism. Overall ANOVA studies indicated that the model was highly significant at a confidence level of 95%. Based on the R2 determination, the model was significant for gram negative bacteria E.coli and Enterobacter aerogenes and the order of significance of model for Gram positive organisms was shown to be B.subtilis > Candida sp. E.coli was the most significantly affected biofilm at 80 µg/ml with a maximum value of 1.217±0.43. B.subtilis biofilm required more amount of nanoparticle to be lysed and showed its maximum at 100 µg/ml(1.705±0.37). Formation of biofilm by gram positive bacteria was prevented effectively than Gram negative bacteria.

Gram positive organisms consist of a thick layer of exopolysaccharides referred to as capsules whereas gram negative cells are surrounded by thin walled cell wall with loosely bound exopolysaccharide called as slime. Though the former sector has a thick layer, the latter forms have multiple layers surrounding the peptidoglycan layer which makes nanoparticles crucial to make entry and destroy EPS. E. coli biofilm was the most significantly inhibited in this study. Limiting biopolymer production by intruding the exopolysaccharide synthesis pathway might also attribute towards biofilm inhibition. Hence manganese nanoparticles exhibited good antibiofilm activity thus concluding that it could serve to eradicating pathogenic biofilms when employed against diseases.

## CONCLUSIONS

The present investigation was an attempt to utilize extracts of *Aegle marmelos* fruit in the synthesis of manganese nanoparticles in a greener way. Isopropanol was capable of extracting most of the phytochemicals which were the prime constituents acting as reducing and capping agents. Characterization studies confirmed that the fabricated product was $MnO_2$ nanoparticles and exhibited definite shape and structure. The smaller size with larger surface area exhibited good biological activities namely antioxidant and antibiofilm activities. Thus, this study revealed that the synthesized $MnO_2$ nanoparticles are potential anti pathogenic materials and since biologically prepared they could be decorated as ecofriendly nanopowder. Further studies could be carried out to perform characterization studies in depth to

identify their salient features and applied broader in the field of biotechnology and pharmaceuticals.

## CONFLICTS OF INTEREST

The authors declare that they have no conflicts of interest regarding the present research article.

## REFERENCES


1. Prabu HJ, Johnson I. Plant-mediated biosynthesis and characterization of silver nanoparticles by leaf extracts of Tragia involucrata, Cymbopogon citronella, Solanum verbascifolium and Tylophora ovata. Karbala International Journal of Modern Science, 2015;1 (4):237-246.
2. Seabra AB, Durán N. Nanotoxicology of metal oxide nanoparticles. Metals, 2015;5 (2):934-975.
3. Rana S, Kalaichelvan P. Antibacterial activities of metal nanoparticles. Antibacterial Activities of Metal Nanoparticles, 2011;11 (02):21-23.
4. Moon SA, Salunke BK, Alkotaini B, Sathiyamoorthi E, Kim BS. Biological synthesis of manganese dioxide nanoparticles by Kalopanax pictus plant extract. IET Nanobiotechnology, 2015;9 (4):220-225.
5. Kumar H, Manisha SP, Sangwan P. Synthesis and characterization of $MnO_2$ nanoparticles using co-precipitation technique. International Journal of Chemistry and Chemical Engineering, 2013;3 (3):155-160.
6. Mittal AK, Chisti Y, Banerjee UC. Synthesis of metallic nanoparticles using plant extracts. Biotechnology advances, 2013;31 (2):346-356.
7. Salunke BK, Sawant SS, Lee S-I, Kim BS. Comparative study of $MnO_2$ nanoparticle synthesis by marine bacterium Saccharophagus degradans and yeast Saccharomyces cerevisiae. Applied microbiology and biotechnology, 2015;99 (13):5419-5427.
8. Dahiya R, Tomar RS, Shrivastava V. Evaluation of Antimicrobial Potential of Aegle Marmelos Fruit Extract against Selected Microorganisms.
9. Kothari S, Mishra V, Bharat S, Tonpay SD. Antimicrobial activity and phytochemical screening of serial extracts from leaves of Aegle marmelos (Linn.). Acta Pol Pharm, 2011;68 (5):687-692.
10. Karumaran S, Nethaji S, Rajakumar R. Antimicrobial and antioxidant activity of leaf extracts of Aegle marmelos.
11. Jayandran M, Haneefa MM, Balasubramanian V. Green synthesis and characterization of Manganese nanoparticles using natural plant extracts and its evaluation of antimicrobial activity. 2015.
12. Murugan K, Krishnasamy S, Kalyanasundaram V, Al-Sohaibani S. Nanotechnological Approach For Exploring The Antibiofilm A Potential Of An Ethanomedicinal Herb Andrographis Paniculata For Controlling Lung Infection Causing Pseudomonas Aeruginosa. Digest Journal of Nanomaterials & Biostructures (DJNB), 2013;8 (1).
13. Liu J, Luo J, Ye H, Sun Y, Lu Z, Zeng X. In vitro and in vivo antioxidant activity of exopolysaccharides from endophytic bacterium Paenibacillus polymyxa EJS-3. Carbohydrate Polymers, 2010;82 (4):1278-1283.
14. Nithya Deva Krupa A, Raghavan V. Biosynthesis of silver nanoparticles using Aegle marmelos (Bael) fruit extract and its application to prevent adhesion of bacteria: a strategy to control microfouling. Bioinorganic chemistry and applications, 2014;2014.
15. Dada A, Adekola F, Odebunmi E. Investigation of the synthesis and characterization of manganese nanoparticles and its ash rice husk supported nanocomposite. Book of Proceedings of 1 st African International Conference/ Workshop on Applications of Nanotechnology to Energy, Health and Environment–March 23 rd–29 th; 2014.
16. Dallas P, Sharma VK, Zboril R. Silver polymeric nanocomposites as advanced antimicrobial agents: classification, synthetic paths, applications, and perspectives. Advances in colloid and interface science, 2011;166 (1):119-135.
17. Kanmani P, Yuvaraj N, Paari K, Pattukumar V, Arul V. Production and purification of a novel exopolysaccharide from lactic acid bacterium Streptococcus phocae PI80 and its functional characteristics activity in vitro. Bioresource Technology, 2011;102 (7):4827-4833.
18. Suriyavathana.M RK. Nanoparticles Synthesis and Antibacterial Study on Anisomeles Malabarica using Manganese Oxide (MnO). International Journal of ChemTech Research, 2015;8 (11):466-473.
19. Rajendran, P. Paramasivam and K.E. Geckeler. Synthesis and Fabrication of Nanomaterials. First Edition. BLOOMSBURY PUBLISHING INDIA PVT. LTD, New Delhi; 2015. 311-4.
20. Sinha A, Singh VN, Mehta BR, Khare SK. Synthesis and characterization of monodispersed orthorhombic manganese oxide nanoparticles produced by Bacillus sp. cells simultaneous to its bioremediation. Journal of hazardous materials, 2011;192 (2):620-627.
21. Shanmugasundaram T, Radhakrishnan M, Gopikrishnan V, Pazhanimurugan R, Balagurunathan R. A study of the bactericidal, anti-biofouling, cytotoxic and antioxidant properties of actinobacterially synthesised silver nanoparticles. Colloids and Surfaces B: Biointerfaces, 2013;111:680-687.
22. Ramamurthy C, Padma M, Mareeswaran R, Suyavaran A, Kumar MS, Premkumar K, Thirunavukkarasu C. The extra cellular synthesis of gold and silver nanoparticles and their free radical scavenging and antibacterial properties. Colloids and Surfaces B: Biointerfaces, 2013;102:808-815.